J. Biochem. 2010;147(4):591–599 doi:10.1093/jb/mvp206

JB THE JOURNAL OF BIOCHEMISTRY

Cloning and characterization of dihydrofolate reductases from deep-sea bacteria

Received November 5, 2009; accepted December 9, 2009; published online December 29, 2009

Chiho Murakami[1], Eiji Ohmae[1,*], Shin-ichi Tate[1], Kunihiko Gekko[1], Kaoru Nakasone[2] and Chiaki Kato[3]

[1]Department of Mathematical and Life Sciences, Graduate School of Science, Hiroshima University, Higashi-Hiroshima 739-8526; [2]Department of Biotechnology and Chemistry, School of Engineering, Kinki University, Higashi-Hiroshima 739-2116; and [3]Marine Biodiversity Research Program, Japan Marine Science and Technology Center (JAMSTEC), Yokosuka 237-0061, Japan

*Eiji Ohmae, Department of Mathematical and Life Sciences, Graduate School of Science, Hiroshima University, Higashi-Hiroshima 739-8526, Japan, Tel/Fax: +81-82-424-7389, E-mail: ohmae@hiroshima-u.ac.jp

Enzymes from organisms living in deep-sea are thought to have characteristic pressure-adaptation mechanisms in structure and function. To better understand these mechanisms in dihydrofolate reductase (DHFR), an essential enzyme in living cells, we cloned, overexpressed and purified four new DHFRs from the deep-sea bacteria *Shewanella violacea* (svDHFR), *Photobacterium profundum* (ppDHFR), *Moritella yayanosii* (myDHFR) and *Moritella japonica* (mjDHFR), and compared their structure and function with those of *Escherichia coli* DHFR (ecDHFR). These deep-sea DHFRs showed 33–56% primary structure identity to ecDHFR while far-ultraviolet circular dichroism and fluorescence spectra suggested that their secondary and tertiary structures were not largely different. The optimal temperature and pH for deep-sea DHFRs activity were lower than those of ecDHFR and different from each other. Deep-sea DHFRs kinetic parameters K_m and k_{cat} were larger than those of ecDHFR, resulting in 1.5–2.8-fold increase of k_{cat}/K_m except for mjDHFR which had a 28-fold decrease. The enzyme activity of ppDHFR and mjDHFR (moderate piezophilic bacteria) as well as ecDHFR decreased as pressure increased, while svDHFR and myDHFR (piezophilic bacteria) showed a significant tolerance to pressure. These results suggest that DHFRs from deep-sea bacteria possess specific enzymatic properties adapted to their life under high pressure.

Keywords: deep-sea bacteria/dihydrofolate reductase/enzyme activity/high-pressure adaptation/molecular evolution.

Abbreviations: DHF, dihydrofolate; DHFR, dihydrofolate reductase; ecDHFR, DHFR from *Escherichia coli*; mjDHFR, DHFR from *Moritella japonica*; myDHFR, DHFR from *Moritella yayanosii*; ppDHFR, DHFR from *Photobacterium profundum*; svDHFR, DHFR from *Shewanella violacea*; THF, tetrahydrofolate.

What underlies the adaptation of microorganisms to deep-sea, an extreme environment with high hydrostatic pressure and low temperature? This question is central to the understanding of their mode of evolution. A large variety of bacteria have been isolated from deep-sea sediments around the world since the first isolation of piezophilic (barophilic) bacteria in 1979 (*1*). *Shewanella violacea* strain DSS12, isolated from the Ryukyu Trench at a depth of 5,110 m, is one of the well-investigated piezophilic bacteria (*2*). This bacterium is an excellent model for studying pressure-adaptation mechanisms because it grows not only at atmospheric pressure but also under high pressure with an optimal growth at 10°C and 30 MPa (*2*, *3*). Genes of this bacterium were analysed and a pressure-regulated promoter was found as an evidence of piezo-adaptation (*4*, *5*). Moreover, it is known that the expression of genes of the respiratory system is regulated by pressure (*6*, *7*), and that an RNA polymerase from this bacterium is more stable and active under higher pressure than the enzyme in *Escherichia coli* (*8*, *9*). *Photobacterium profundum* strain SS9, isolated from the Sulu Sea at a depth of 2,551 m, is a moderate piezophilic bacterium growing over a wide pressure range of up to 90 MPa with an optimal growth at 15°C and 28 MPa (*10–14*). Pressure response of this bacterium is characterized by modulations of gene expression and protein abundance (*15–18*). Recently, the whole genome sequence of this bacterium was determined (*19*), allowing for a genetic investigation of the pressure-adaptation mechanisms. *Moritella yayanosii* strain DB21MT-5 was isolated from the Mariana Trench at a depth of 10,898 m as the first species of hyperpiezophilic bacterium of the genus *Moritella* (*20*). This bacterium cannot grow below 30 MPa but grows well under pressures of 60–100 MPa, with an optimal condition of 80 MPa and 10°C (*21*). *Moritella japonica* strain DSK1, isolated from the Japan Trench at a depth of 6,356 m, is a piezotolerant bacterium with an optimal growth at 0.1 MPa and 10°C (*22*).

The pressure-adaptation mechanisms of these deep-sea bacteria have mostly been studied through gene regulatory analyses, while protein adaptations have not yet been sufficiently explored. Indeed, experimental difficulties have limited the characterization of deep-sea bacteria proteins: their expression and purification are generally hindered by their altered stabilities under atmospheric pressure. Therefore, only few reports are available on the characterization of deep-sea bacterial proteins, including cytochrome *c* from *S. violacea* strain DSS12 (*23*) and malate dehydrogenases from some bacteria (*24*).

Proteins from deep-sea bacteria should have different structural and functional features compared with orthologous proteins from bacteria living at atmospheric pressure. The comparative study of proteins found in both deep-sea and atmospheric pressure bacteria should therefore provide important insights into pressure-adaptation mechanisms by which proteins maintain their function under the unusually high pressure and low temperature found in deep-sea.

Dihydrofolate reductase (DHFR) is an excellent target enzyme for such purpose because it is an essential enzyme in all living cells. DHFR catalyses the NADPH-dependent reduction of dihydrofolate (DHF) to tetrahydrofolate (THF), which is a precursor of an important cofactor for the biosynthesis of purine nucleotides and some amino acids. It is known that DHFR from *E. coli* (ecDHFR) living at atmospheric pressure is highly flexible and that its structure and function are sensitive to pressure (*25*, *26*). Recently, we found that the activity of ecDHFR decreases with increasing pressure, whereas DHFR from *S. violacea* DSS12 (svDHFR) has an optimal activity at ~100 MPa (*27*). These findings suggest that DHFRs from deep-sea bacteria (hereafter, abbreviated as deep-sea DHFRs) have characteristic pressure susceptibilities and structural dynamics different from those of organisms living at atmospheric pressure.

In this work, we compared the structure and enzymatic properties of ecDHFR with those of newly isolated DHFRs from the deep-sea bacteria *S. violacea* strain DSS12 (svDHFR), *P. profundum* strain SS9 (ppDHFR), *M. yayanosii* strain DB21MT-5 (myDHFR) and *M. japonica* strain DSK1 (mjDHFR). Based on these comparisons, we discuss the pressure-adaptation mechanisms of DHFR.

Materials and Methods

Cloning and construction of deep-sea DHFRs overexpression plasmids

Construction of the svDHFR overexpression plasmid was described previously (*27*). Genomic DNAs of *P. profundum* strain SS9, *M. yayanosii* strain DB21MT-5 and *M. japonica* strain DSK1, which were kindly provided by Dr Nogi from JAMSTEC, were digested with PstI, EcoRI and HincII, respectively. Resulting DNA fragments were ligated to pUC118 vectors digested with PstI, EcoRI or SmaI, and transformed into *E. coli* HB101 competent cells (TAKARA BIO, Otsu, Japan). The transformants carrying deep-sea DHFR genes were selected at 25°C on LB-plates containing ampicillin (100 μg/ml) and trimethoprim (5 μg/ml). The plasmids were then purified and *in vitro* insertion of a kanamycin-resistant gene was carried out using a Gene Jumper kit (Invitrogen, Carlsbad, CA, USA). The obtained plasmids were transformed into *E. coli* Top10 competent cells (Invitrogen, Carlsbad, CA, USA) and trimethoprim-sensitive revertants were selected from colonies of transformants formed on LB-plates containing ampicillin (100 μg/ml) and kanamycin (20 μg/ml). The plasmids from the revertants were purified, and both up- and down-streams of its insert were sequenced using a DYEnamic ET terminator cycle sequencing kit (GE Healthcare UK Ltd., Buckinghamshire, UK) and an ABI prism 310 genetic analyzer (Applied Biosystems, Foster City, CA, USA). The sequences were registered in DDBJ/GenBank/EMBL databases under accession Nos. AB519243, AB505966, AB505967 and AB505968 for svDHFR, ppDHFR, myDHFR and mjDHFR, respectively.

DHFR genes were amplified by PCR using primers listed in Table I and a KOD-Plus-DNA polymerase (TOYOBO, Osaka, Japan), and then ligated to pUC118 vectors digested with SmaI and transformed into *E. coli* HB101 competent cells. The overexpressed transformants were selected at 37°C on LB-plates containing ampicillin (100 μg/ml) and trimethoprim (20 μg/ml). The DNA sequence of the overexpression plasmids was determined as described above.

Table I. Oligonucleotide primers used in PCR amplification of deep-sea DHFR genes from *P. profundum*, *M. yayanosii* and *M. japonica*.

Primer	Sequence
ppDHFR-F	5′-AGGAACTTCCATGATCGCAGCTATGGCTAA-3′
ppDHFR-R	5′-GAGGATCCTTAAGTAAGATCGACGTTACGT-3′
myDHFR-F	5′-AGGAACTTCCATGATTGCCGCACTGGCAAA-3′
myDHFR-R	5′-GAGGATCCCTACTTCACTCGCTCGAGTAAA-3′
mjDHFR-F	5′-AGGAACTTCCATGAAGTTATCATTAATGGC-3′
mjDHFR-R	5′-GAGGATCCTTAACTATTTTGCCAAATTTGA-3′

Protein purification

ecDHFR was purified from *E. coli* HB101 cells as described previously (*28*). Deep-sea DHFRs were expressed in *E. coli* as inclusion bodies at 37°C and in the soluble fraction at 25°C. Therefore, except for mjDHFR, the purification method of deep-sea DHFRs was essentially the same as that of ecDHFR. Cells were grown for 48 h at 25°C, harvested by centrifugation, washed with 20 mM Tris–HCl (pH 8.0) containing 14 mM 2-mercaptoethanol and 0.1 mM EDTA (buffer A), and broken by sonication. Then, 2% (wt/vol) streptomycin sulphate was added to the soluble fraction to precipitate nucleic acids. After centrifugation, supernatant from the 45% saturated ammonium sulphate fraction was loaded on a methotrexate–agarose affinity column (3 × 10 cm) (Sigma-Aldrich, St. Louis, MO, USA) equilibrated with buffer A. The column was washed with buffer A containing 0.5 M NaCl and the DHFR protein was eluted with buffer A containing 3 mM folate. DHFR-containing fractions were dialysed against 20 mM Tris–HCl (pH 9.0) containing 14 mM 2-mercaptoethanol and 0.1 mM EDTA (buffer B) and concentrated with a DE-52 anion-exchange column (1 × 5 cm) (Whatman, Kent, UK). The samples were then dialysed against buffer B containing 3M guanidine hydrochloride to completely remove the folate and against buffer B containing 6 M urea to completely remove the guanidine hydrochloride. Proteins were then refolded by dilution with buffer B to a concentration of ~10 μM. Refolded DHFRs were dialysed against 20 mM Tris–HCl (pH 8.0) containing 0.1 mM dithiothreitol and 0.1 mM EDTA (buffer C) and concentrated with an Amicon Ultra filter (Millipore, Billerica, MA, USA). The aggregates were removed by centrifugation.

Since the affinity of mjDHFR for the methotrexate–agarose resin was very low, it was purified using anion-exchange, hydroxyapatite and gel-permeation chromatography. The supernatant from the 45% saturated ammonium sulphate fraction was dialysed against buffer A containing 20% glycerol and loaded on a DE-52 column (3 × 10 cm). Proteins were eluted by a linear-gradient of NaCl from 0 to 0.5 M. After dialysis of the fractions containing mjDHFR against 10 mM potassium phosphate (pH 8.0) containing 14 mM 2-mercaptoethanol, 0.1 mM EDTA and 20% glycerol, the samples were loaded on a hydroxyapatite column (2 × 10 cm) (Bio-Rad, Hercules, CA, USA) pre-equilibrated with the same buffer. Since mjDHFR does not bind to the resin, the flow-through of the column was collected and dialysed against buffer A containing 20% glycerol. Finally, the sample was concentrated with an Amicon Ultra filter and loaded on a Sephadex G-75 column (3 × 80 cm) (Amersham Biosciences UK Ltd, Buckinghamshire, UK). Because mjDHFR was not effectively refolded by the above method and had no folate as judged from the absorbance spectrum, the purified mjDHFR was only concentrated with an Amicon Ultra filter and dialysed against buffer C containing 20% glycerol because enzyme activity was lost after dialysis against buffers without glycerol. Consequently, a trace of glycerol (<0.2%) remained in the mjDHFR samples used in all experiments.

The concentration of ecDHFR was determined from its absorbance at 280 nm using a molar extinction coefficient of 31,100 $M^{-1} cm^{-1}$ (*29*). The protein concentrations of svDHFR,

myDHFR, ppDHFR and mjDHFR were determined using molar extinction coefficients of 22,900, 29,900, 26,000 and 17,400 $M^{-1}\,cm^{-1}$ at 280 nm, respectively, which were estimated from the fluorescence intensities of the fully unfolded DHFRs in 6 M guanidine hydrochloride solutions.

Circular dichroism spectrometry

Far-ultraviolet circular dichroism (CD) spectra of DHFRs were measured using a Jasco J-720W spectropolarimeter. The temperature was maintained at 15°C using a Peltier-controlled thermobath (Jasco PTC-348W). The solvent used was 20 mM Tris–HCl (pH 8.0) containing 0.1 mM EDTA and 0.1 mM dithiothreitol. The protein concentration was 10 μM.

Fluorescence spectrometry

Fluorescence spectra of DHFRs were measured at 15°C using a Jasco FP-750 spectrofluorometer with an excitation wavelength of 290 nm and an emission wavelength of 300–450 nm. The solvent used was the same as in the CD measurements. The protein concentration was 0.3–0.8 μM and the intensities of the spectra were normalized at 1 μM protein.

Enzyme assay at atmospheric pressure

The enzyme activity of DHFRs at atmospheric pressure was assayed with a Jasco V-560 spectrophotometer. The solvent used was 20 mM Tris–HCl (pH 7.0) containing 0.1 mM EDTA and 0.1 mM dithiothreitol. The concentrations of DHF (Sigma-Aldrich, St Louis, MO, USA) and NADPH (Oriental Yeast, Tokyo, Japan) were determined spectrophotometrically using molar extinction coefficients of 28,000 $M^{-1}\,cm^{-1}$ at 282 nm for DHF and 6,200 $M^{-1}\,cm^{-1}$ at 339 nm for NADPH (*30*). The enzymatic reaction was started by mixing the DHF solution with the enzyme–NADPH solution at final concentrations of 1–2 nM DHFR, 50 μM NADPH and 50 μM DHF. Before mixing, both solutions were preincubated for 10 min to equilibrate the temperature and eliminate the hysteresis effect (*31*). The initial velocity of the enzymatic reaction was calculated from the time course of absorbance at 340 nm with a differential molar extinction coefficient of 11,800 $M^{-1}\,cm^{-1}$ (*32*). The effect of the temperature on the enzymatic reaction was examined in a range of 5–65°C in a circulating thermobath (NESLAB RTE-5). The pH dependence of the enzymatic reaction was examined at pHs from 5.0 to 9.5 at 25°C.

Steady-state kinetics at atmospheric pressure

Steady-state kinetics of the enzymatic reaction was measured using the same procedure and solvent as in the above enzymatic assay. The enzymatic reaction was measured under various concentrations of NADPH or DHF while maintaining the constant ligand at a saturating concentration of 50 μM (except for myDHFR and mjDHFR where we used 500 μM with a cell of 5 mm light-pass length). In both experiments, the enzyme concentration was 1–8 nM. The concentration of DHFRs was determined by a methotrexate titration method (*33*) except for mjDHFR, which was determined spectrophotometrically because of its low affinity to methotrexate. The initial velocity of the enzymatic reaction was calculated as in the enzymatic assay except for myDHFR and mjDHFR where we used a differential molar extinction coefficient of 3,180 $M^{-1}\,cm^{-1}$ at 370 nm (*26*) because the absorbance at 340 nm was too high to measure the reaction. The Michaelis (K_m) and catalytic (k_{cat}) constants were determined with the program Origin (OriginLab, Northampton, MA, USA) by direct fitting of the initial velocity of the enzymatic reaction on the Michaelis–Menten equation using a non-linear least-squares regression analysis.

Enzyme assay under high pressures

Pressure dependence of the enzyme activity was measured with a Jasco V-560 spectrophotometer equipped with a high-pressure absorbance cell unit (Teramecs PCI-400) and a hand pump (Teramecs PCI-500) as described previously (*26*). Temperature was maintained at 25°C with a circulating thermobath (NESLAB RTE-5). The buffer used was 20 mM Tris–HCl (pH 7.0) containing 0.1 mM EDTA, 0.1 mM dithiothreitol, 250 μM NADPH and 250 μM DHF. The reaction mixture containing DHF and the enzyme–NADPH solution was loaded in the high-pressure cell, and the absorbance at 370 nm was measured for 1–5 min at the desired pressure. The initial velocity of the enzymatic reaction was calculated from the time course of the absorbance using the differential molar extinction coefficient at each pressure (e.g. 3,180 and 3,710 $M^{-1}\,cm^{-1}$ at 0.1 and 250 MPa, respectively). The initial velocities from two to four independent measurements were averaged at each pressure. The activation free energy (ΔG^*) and the activation volume (ΔV^*) of the enzymatic reaction were calculated using the following equation, which is applicable at saturating substrate concentrations

$$\Delta V^* = \partial \Delta G^*/\partial P = \partial(-RT\ln k_{cat})/\partial P = \partial(-RT\ln v)/\partial P, \quad (1)$$

where R is the gas constant, T is the temperature, P is the pressure and v is the initial velocity of the enzymatic reaction (*26*).

Results and discussion

Amino acid sequences of deep-sea DHFRs

The alignment of svDHFR, ppDHFR, myDHFR and mjDHFR putative amino acid sequences are presented in Fig. 1. Sequence identities to ecDHFR for svDHFR, ppDHFR, myDHFR and mjDHFR were 55, 56, 55 and 33%, respectively. Overall, the N-terminal regions, particularly up to residue 60, show high sequence conservations, while the C-terminal regions show sequence variations among DHFRs. The Gly95–Gly96 residues, known to be essential for the folding of ecDHFR, were also completely conserved in all deep-sea DHFRs. Moreover, many residues in the binding site of the substrate (Ala6, Ala7, Trp22, Phe31, Lys32, Leu54 and Arg58) and the cofactor (Ala6, Ala7, Ile14, Gly15, Arg44, Thr46, Ser63, Gly95, Gly96 and Tyr100) were fully conserved in all DHFRs (Fig. 1). The Met20 loop comprising residues 10–24, which is a well-characterized functionally essential region, is also conserved in sequence among DHFRs.

Among the above deep-sea DHFRs, mjDHFR shows the lowest sequence identity to ecDHFR (33%, Fig. 1). Several residues in the substrate binding sites were changed in mjDHFR compared with those in ecDHFR: Ile5, Glu17, Met20, Leu28, Ile50, Ile94 and Thr113 in ecDHFR were, respectively, changed to Met5, Gly17, Ile20, Gln28, Met50, Val94 and Ser113 in mjDHFR. Noticeably, the Glu17 and Leu28 substitutions are conserved in the other DHFRs shown in Fig. 1, which might explain the lower substrate affinity of mjDHFR shown in Table II and discussed below.

Deep-sea DHFRs were purified and predominantly gave single bands on a SDS-PAGE (Fig. 2). The mass spectroscopic data indicate that all purified DHFR proteins from deep-sea bacteria have an additional 14 residues (MTMITNSSSVPGTS) in the N-terminal region, which originate from a vector *lac*Z' gene. The expression of the enzymes was significantly decreased after elimination of these residues probably due to unstable structure. Then, we used deep-sea DHFRs with these additional residues in all experiments.

Structure of deep-sea DHFRs

Figure 3A shows the far-ultraviolet CD spectra of deep-sea DHFRs and ecDHFR at 15°C and pH 8.0. CD spectra of deep-sea DHFRs were largely blue-shifted relative to that of ecDHFR and accompanied by small changes in peak intensities. These modified CD spectra do not necessarily mean that the

```
                10        20        30        40        50        60
ecDHFR     -MISLIAALAV DRVIGMENAM PWNLPADLAW FKRNTLNKPV IMGRHTWESI GRPLPGRKNI
svDHFR     MKIAMIAAMAN NRVIGKDNQM PWHLPEDLKH FKAMTLGKPI VMGRKTYDSI GRALPGRLNI
ppDHFR     ----MIAAMAK DRVIGKDNAM PWHLPADFAW FKKSTLGKPI VMGRKTFESI GRPLPGRLNI
myDHFR     ----MIAALAN NRVIGLDNKM PWHLPAELQL FKRATLGKPI VMGRNTFESI GRPLPGRLNI
mjDHFR     MKLSLMAAKSK NGVIGNGPDI PWQAKGEQLL FKAMTYNQWL LVGRKTFESM G-TLPNRKYA
               ::** :  : ***    : **:   :    **  * .: : ::**:*::*: * .**.*

                70        80        90        100       110       120
ecDHFR     ILSSQP-GT-DD RVTWVKSVDE AIAACGDVPE IMVI-GGGRVY EQFLPKAQKL YLTHIDAEVE
svDHFR     VISRQEGLS-IP GVTCVTSFEM AVEAAGECEE LVVI-GGGQLY ASLLSKADKL YLTEINLDVA
ppDHFR     VISRNPEFS-VE GVTVVADIEA AKHAAGDIGE LMVI-GGGSIY EACLPSADRL YLTFIDLDVD
myDHFR     VLSRQTDYQ-PE GVTVVATLED AVVAAGDVEE LMII-GGATIY NQYLAAADRL YLTHIELTIE
mjDHFR     VISRSDFVSEDE NVMVFSSIES ALRQLADITD HVIVSGGGEIY RSLISKVDTL HISTIDIETE
           ::*.          *  .  .:  *    .:  :  ::: **. :*    :. . : * ::: *:

                130       140       150       160       Residues   Identity
ecDHFR     GDTHFPDYEP DDWESVFSEF HDADAQNSHS YCFEILERR- ---     159       100.0%
svDHFR     GDTFFPQWDD GSWERISQEM LVNGAG--LE YSFINLVKKC ---     160        54.7%
ppDHFR     GDTCFPDWGE G-WIKSYTEH YSADEKNAHD MQFVILERNV DLT     160        55.8%
myDHFR     GDTWFPDYEQ YHWQEIEHES YAADDKNPHD YRFSLLERVK ---     158        55.1%
mjDHFR     GDIVFPDIPD SFSLAFEQKF ESN-----IN YCYQIWQNS- ---     157        33.1%
           **  **:          :              .   :   .
```

Fig. 1 Comparison of DHFR amino acid sequences from *E. coli* and four deep-sea bacteria. Multiple alignments were conducted with the CLUSTALW program (*43*) on a server from the DNA Data Bank of Japan (http://www.ddbj.nig.ac.jp/). Numbering of residues is based on the ecDHFR sequence. The symbols 'asterisk', 'colon' and 'end point' below the alignment, indicate fully, strongly and weakly conserved residues, respectively. Amino acid residues that contact with the substrate and the cofactor in the crystal structure of ecDHFR–$NADP^+$–folate ternary complex (*44*) are indicated by open and gray boxes, respectively. Sequence lengths and levels of identity to ecDHFR are also indicated at the end of each sequence.

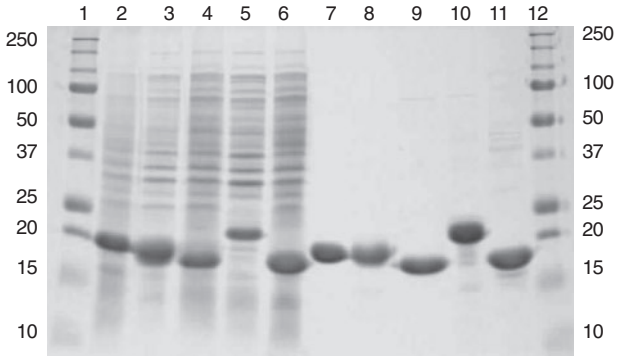

Fig. 2 SDS–PAGE of *E. coli* and deep-sea bacteria DHFRs. Lanes 1 and 12: molecular weight markers. Lanes 2–6: whole protein extracts from *E. coli* containing the overexpressed ecDHFR, svDHFR, ppDHFR, myDHFR and mjDHFR. Lanes 7–11: purified ecDHFR, svDHFR, ppDHFR, myDHFR and mjDHFR.

secondary structures of deep-sea DHFRs are different from that of ecDHFR because single amino acid substitutions in ecDHFR can induce large changes in CD spectrum (*28*, *34–36*). Similar instances have also been reported by other groups (*37*, *38*). Such large CD changes may rather be ascribed to the highly flexible structure of DHFR, which could perturb the CD excitation through movements of the secondary structure and/or altered contributions of aromatic side chains typically induced by an exciton coupling of Trp47 and Trp74 in ecDHFR (*35*, *37*). The finding that no significant difference in CD spectra was induced by addition of cofactor (NADPH) and substrate (DHF) (Fig. 3A, inset) confirms that these deep-sea apo-DHFRs are in a folded (native) conformation although they carry 14 additional residues in the N-terminal region.

Figure 3B shows the fluorescence spectra of deep-sea DHFRs and ecDHFR at 15°C and pH 8.0. The fluorescence spectra were mainly attributable to the content and environment of the tryptophan residues in the proteins. svDHFR, myDHFR and mjDHFR, with three tryptophan residues, show reduced peak intensities compared with ecDHFR, which has five tryptophan residues. Small blue shifts of peak wavelength from 345 to 340–343 nm suggest that their tryptophan residues existed in more hydrophobic environments than those of ecDHFR. ppDHFR for its part showed an oppositely red-shifted peak at 348 nm accompanied by a similarly reduced intensity although this protein has four tryptophan residues. These results suggest that the quantum yield of tryptophan residues and the polarity around them are considerably different within each DHFR.

Taken together, the spectral data of the deep-sea DHFRs studied here indicate that the enzymes have not experienced global structural changes but have retained somewhat local structural alterations, as evidenced by changes in their CD and fluorescence spectra compared with those of ecDHFR. These observations are confirmed by the fact that deep-sea DHFRs retained enzymatic activities comparable to that of ecDHFR, as shown below.

Recently, we determined the crystal structure of the DHFR–$NADP^+$–folate ternary complex of DHFR from another deep-sea bacterium *M. profunda* (Hata *et al.*, unpublished), which has a 55% sequence identity with ecDHFR (*39*). Others have also reported the crystal structure of the apo form and DHFR–NADPH–MTX ternary complex of the same protein (*40*). These results are consistent with the interpretation that the deep-sea DHFR has only marginal structural differences compared with ecDHFR, which

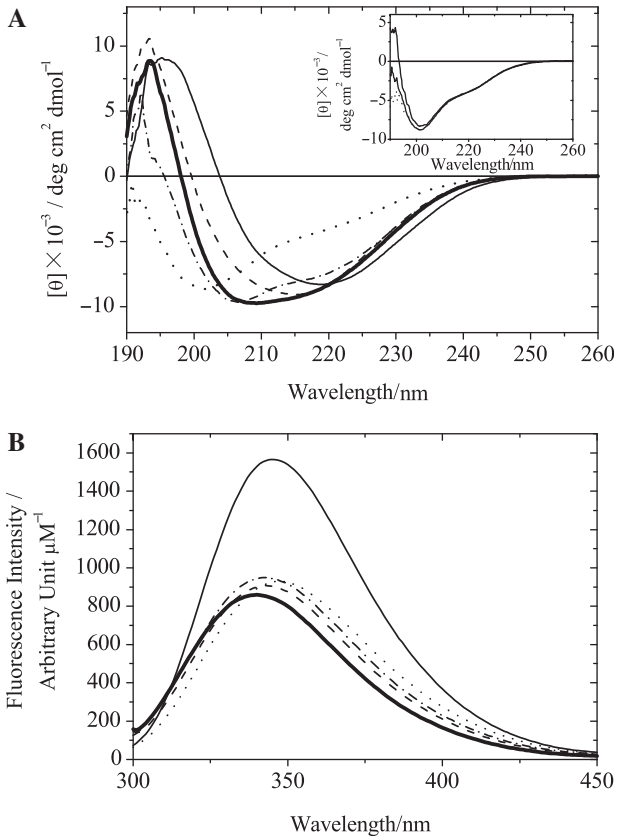

Fig. 3 Far-ultraviolet CD (A) and fluorescence (B) spectra of *E. coli* and deep-sea bacteria DHFRs at pH 7.0 and 15°C. The solvent used was 20 mM Tris–HCl containing 0.1 mM EDTA and 0.1 mM dithiothreitol. Continuous line: ecDHFR, dashed line: svDHFR, dotted line: ppDHFR, dashed and dotted line: myDHFR, and thick line: mjDHFR. Inset of panel A: far-ultraviolet CD spectra of ppDHFR with or without ligands. Continuous line: apo-ppDHFR, dashed line: ppDHFR with 250 μM NADPH and thin solid line: ppDHFR with 250 μM dihydrofolate.

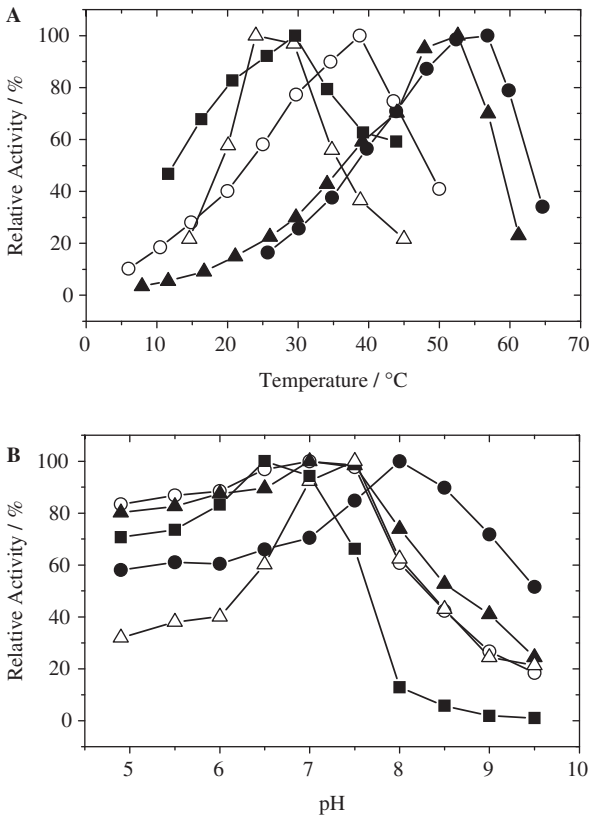

Fig. 4 Temperature (A) and pH (B) dependences of the enzyme activity of *E. coli* and deep-sea bacteria DHFRs. The solvent used was 20 mM Tris–HCl containing 0.1 mM EDTA, 0.1 mM dithiothreitol, 50 μM NADPH and 50 μM dihydrofolate. Filled circle: ecDHFR, open circle: svDHFR, filled triangle: ppDHFR, open triangle: myDHFR and filled square: mjDHFR.

further supports our spectroscopic observations mentioned above.

Enzyme function of deep-sea DHFRs at atmospheric pressure

To characterize the enzyme function of deep-sea DHFRs, we examined the effects of temperature and pH on enzyme activity. Figure 4A shows the temperature dependence of ecDHFR and deep-sea DHFRs at pH 7.0 and 0.1 MPa. Under these experimental conditions, the optimal temperatures of myDHFR, mjDHFR svDHFR, ppDHFR and ecDHFR were ~25, 30, 40, 53 and 57°C, respectively. The low optimal temperatures of deep-sea DHFRs compared with ecDHFR suggest a decreased thermal stability of these proteins although these optimal temperatures have no correlation with the optimal growth temperature of each bacterium.

Figure 4B shows the pH dependence of ecDHFR and deep-sea DHFRs at 25°C and 0.1 MPa. The optimal pHs of mjDHFR, svDHFR, ppDHFR, myDHFR and ecDHFR were ~6.5, 7.0, 7.0, 7.5 and 8.0, respectively. The catalytic residue Asp27 of ecDHFR was conserved in svDHFR and ppDHFR, and replaced by glutamate in myDHFR and mjDHFR (Fig. 1). Because of the similar chemical characteristics of Glu and Asp, the residues should have a similar role as a proton source in the hydride transfer process described in ecDHFR (*41*). However, the observed differences in pH dependencies cannot be explained without detailed structural analyses because they can stem from various sources including variations in the rate-limiting product-releasing step and alterations of the local environments surrounding the catalytically essential residues Asp27 or Glu27 in the hydride transfer process.

To further clarify the catalytic reaction of deep-sea DHFRs, the steady-state enzyme kinetics was examined at pH 7.0 and 25°C. The measured kinetic parameters K_m and k_{cat} for ecDHFR and deep-sea DHFRs are listed in Table II. The K_m values of myDHFR, svDHFR and ppDHFR for DHF were 1.5–5.1-fold larger than that of ecDHFR whereas the K_m was significantly larger (216-fold) for mjDHFR. The k_{cat} values of the four deep-sea DHFRs were 4.6–8.5-fold larger than that of ecDHFR, resulting in 1.5–2.8-fold increases in k_{cat}/K_m with an exceptionally large decrease (28-fold) for mjDHFR. Thus, myDHFR, svDHFR and ppDHFR are more active than ecDHFR because of the large turn-over rate that overcomes the diminished affinity for the substrate, whereas mjDHFR is less active mainly because of the severely reduced substrate binding ability.

Table II. Steady-state kinetic parameters of ecDHFR and deep-sea DHFR enzymatic reactions at 25°C and pH 7.0 under atmospheric pressure[a].

	DHF			NADPH		
DHFRs	K_m (μM)	k_{cat} (s^{-1})	k_{cat}/K_m ($\mu M^{-1} s^{-1}$)	K_m (μM)	k_{cat} (s^{-1})	k_{cat}/K_m ($\mu M^{-1} s^{-1}$)
ecDHFR	1.1 ± 0.1	18.4 ± 0.2	16.7 ± 1.7	1.9 ± 0.0	19.2 ± 0.1	10.1 ± 0.1
svDHFR	1.9 ± 0.2	90.1 ± 2.9	47.4 ± 6.5	3.4 ± 0.3	86.8 ± 2.0	25.5 ± 2.8
ppDHFR	6.2 ± 0.8	156.0 ± 5.6	25.2 ± 4.2	19.8 ± 0.8	150.5 ± 2.3	7.6 ± 0.4
myDHFR	1.8 ± 0.2	83.8 ± 2.4	46.6 ± 6.5	101.1 ± 9.9	80.3 ± 3.4	0.8 ± 0.1
mjDHFR	238 ± 26	144.5 ± 3.2	0.6 ± 0.1	58.4 ± 1.9	109.2 ± 1.1	1.9 ± 0.1

[a]The buffer used was 20 mM Tris–HCl (pH 7.0) containing 0.1 mM EDTA and 0.1 mM dithiothreitol.

Increases in K_m and k_{cat} (up to 53- and 7.8-fold, respectively) were also observed for NADPH (Table II). Thus, deep-sea DHFRs have a lower affinity than ecDHFR for both substrate and cofactor, and an increased turn-over rate. Changes in deep-sea DHFRs k_{cat} are comparable to NADPH and DHF, although the k_{cat} value of mjDHFR may be slightly smaller because the concentration of DHF (500 μM) was not saturating. In contrast, changes in deep-sea DHFRs K_m are not necessarily comparable to NADPH and DHF. The K_m value of NADPH is larger than that of DHF for myDHFR while it is the opposite for mjDHFR. The significantly decreased affinity of mjDHFR for DHF and NADPH might be due to the large quantity of amino acid substitutions found in the binding sites of this DHFR although this explanation is only partial since residues in the binding sites of myDHFR, ppDHFR and svDHFR are almost identical to those of ecDHFR (Fig. 1) but their affinity for the ligand is lower than that of ecDHFR.

Pressure effect on enzyme activity

Figure 5A shows the relative activity of DHFRs as a function of the hydrostatic pressure at pH 7.0 and 25°C. ecDHFR and ppDHFR showed a monotonous decrease of their activities with increasing pressure, down to ~50 and 20% at 250 MPa, respectively. mjDHFR lost the activity significantly even in the low-pressure region and almost completely above 100 MPa, which may be related to its low substrate-binding ability (Table II). On the other hand, the enzymatic activity of svDHFR increased with pressure to ~110% at around 75 MPa and then decreased to ~60% at 250 MPa. This feature is consistent with our previous result although the maximal activity is slightly different (*27*). myDHFR also showed the similar pressure-resistant activity: the activity was invariant below 75 MPa and then gradually decreased with increasing pressure down to ~30% at 250 MPa. These results indicate that deep-sea DHFRs have specific characteristics in enzyme kinetics and structural fluctuation to adapt to deep-sea conditions.

The activation free energy (ΔG^*) calculated using Eq. (*1*) and the data from Fig. 5A is plotted against pressure in Fig. 5B. Expectedly, there is a good linear relationship between ΔG^* and pressure for ecDHFR, ppDHFR and mjDHFR while two other deep-sea DHFRs show a bimodal linear relationship with an

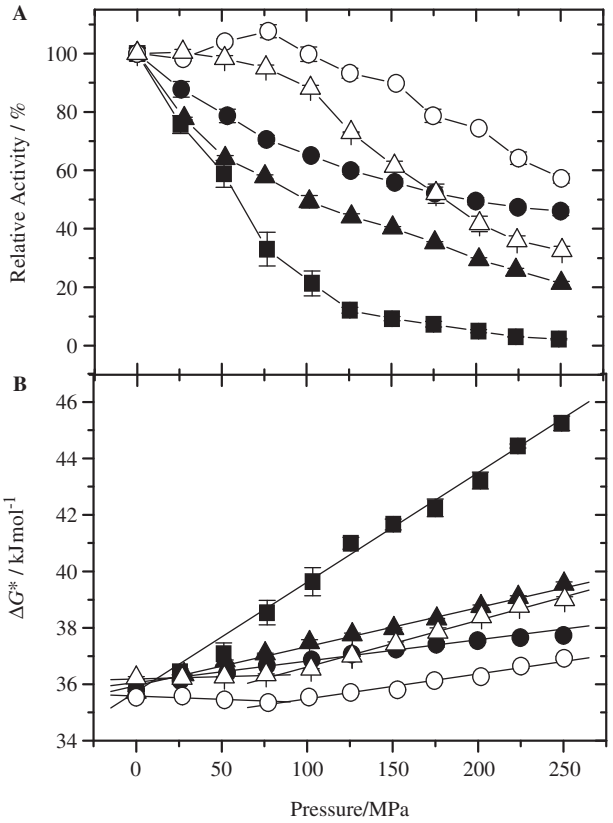

Fig. 5 Pressure dependence of relative enzyme activities (A) and activation free energies (B) of *E. coli* and deep-sea bacteria DHFRs at pH 7.0 and 25°C. The solvent used was 20 mM Tris–HCl (pH 7.0) containing 0.1 mM EDTA, 0.1 mM dithiothreitol, 250 μM NADPH and 250 μM dihydrofolate. Filled circle: ecDHFR, open circle: svDHFR, filled triangle: ppDHFR, open triangle: myDHFR and filled square: mjDHFR. Lines in panel B were drawn using least-squares linear regression.

intersection at ~75 MPa. The activation volumes (ΔV^*) of the enzymatic reactions calculated from these slopes are listed in Table III. Positive ΔV^* values indicate that the activated state has a larger partial volume than the reactant in the rate-limiting process of the enzymatic reaction, resulting in the pressure-induced depression of this process. The ΔV^* value of 7.5 ± 0.2 ml/mol calculated for ecDHFR accurately matches that of 7.6 ± 0.8 ml/mol previously published (*26*). All these deep-sea DHFRs show larger ΔV^* values (1.2–5.2-fold) than ecDHFR although svDHFR and myDHFR have negative or negligibly small positive ΔV^* values at pressures below

Table III. Activation volumes of ecDHFR and deep-sea DHFR enzymatic reactions at 25°C and pH 7.0[a].

DHFRs	ΔV^* (ml mol^{-1})[b]	
ecDHFR	7.5 ± 0.2 (0.1–250 MPa)	
svDHFR	–2.7 ± 1.1 (0.1–75 MPa)	8.9 ± 0.6 (75–250 MPa)
ppDHFR	13.8 ± 0.1 (0.1–250 MPa)	
myDHFR	1.7 ± 0.6 (0.1–75 MPa)	16.5 ± 0.6 (75–250 MPa)
mjDHFR	38.7 ± 0.3 (0.1–250 MPa)	

[a]The buffer used was 20 mM Tris–HCl (pH 7.0) containing 0.1 mM EDTA, 0.1 mM dithiothreitol, 250 μM NADPH and 250 μM DHF. [b]The values in parenthesis indicate pressure range used for calculation.

75 MPa. The quantitative analysis of these ΔV^* values is limited because the enzyme kinetics and the structure of deep-sea DHFRs are unknown. Nevertheless, these volumetric data clearly demonstrate the pressure-dependent function of deep-sea DHFRs.

The steady-state kinetics under high pressures was not examined in the present study due to technical difficulties. However, the distinctive pressure-dependent enzymatic activity is worth discussing based on the enzyme kinetics and structure of ecDHFR, because five steps (binding of substrate and cofactor, hydride transfer, and releasing of two products) should be essential for the catalytic reaction of all DHFRs although the order of these steps may differ between DHFRs from different species. ecDHFR catalyses the NADPH-linked reduction of DHF to THF through a cycle of five intermediate states (DHFR-NADPH → DHFR-NADPH-DHF → DHFR-NADP$^+$-THF → DHFR-THF → DHFR-NADPH-THF) involving equilibrium states such as DHFR–NADP$^+$. The ternary complex DHFR–NADPH–DHF exists only transiently because the hydride transfer from NADPH to DHF is very rapid. In these processes, the rate-limiting step at atmospheric pressure is the release of the product (THF) from the ternary complex (DHFR–NADPH–THF) (*29*). It is probable that the enzyme kinetics of deep-sea DHFRs follows that of ecDHFR, judging from the conserved amino acid residues in the active sites (Fig. 1) and the comparable kinetic data at atmospheric pressure (Table II). Recently, we determined the volume levels of the kinetic intermediates of ecDHFR (*26*). We found that the hydride transfer was not the rate-limiting process under high pressure, and predicted three candidates for the rate-limiting process of the enzymatic reaction: two are the releasing processes of THF and NADP$^+$, and the third is the conformational transition of the enzyme. Others also reported that the hydride transfer was not the rate-limiting process under high pressure for another deep-sea DHFR from *M. profunda* (*40*). The binding steps of DHF and NADPH could also be eliminated from candidates of the rate-limiting step under high pressure, because the concentrations of the substrate and cofactor used for the high-pressure experiments were much higher than the K_m values except for mjDHFR. However considering the comparable ΔV^* values obtained for ecDHFR, svDHFR, ppDHFR and myDHFR (Table III), any of these three candidates could be the rate-limiting process for svDHFR, ppDHFR and myDHFR under high pressure while some other contribution might be involved in mjDHFR large ΔV^* value.

There are lines of evidence for a conformational change of ecDHFR under high pressure. For example, the free energy change of the ligand binding to ecDHFR showed different pressure dependences below and above ~50 MPa, suggesting that some conformational change of the enzyme occurs at pressures above 50 MPa (*26*). A high-pressure NMR study also revealed the presence of two conformers, 'closed' and 'open', in ecDHFR–folate complex whose relative occurrences were sensitively influenced by pressure (*25*). This suggests that such a conformational change of the enzyme also occurs in the transient state DHFR–NADPH–DHF. Cameron and Benkovic (*42*) have reported that the conformational conversion in DHFR–NADPH–DHF is the rate-limiting step for the G121V mutant of ecDHFR. Although it is unknown whether this conformational conversion is identical to the transformation from 'open' to 'closed' conformer and if it also occurs in deep-sea DHFRs, it is still possible that the conformational change of the enzyme under high pressure is the rate-limiting step at least in the case of svDHFR and myDHFR, which have shown a pressure-resistant activity.

Another important problem is the structural fluctuation of the enzyme. The fact that most deep-sea DHFRs were isolated as inclusion bodies in *E. coli* cells grown at 37°C suggests that the structure of these proteins is highly flexible and easily unfolded during expression. Such flexible structure could easily be compressed by pressure to a rigid conformation diminishing the enzyme activity (like ppDHFR and mjDHFR) or to a more desirable conformation increasing the functionality in an optimal pressure range while the enzyme activity would still be decreased by a very rigid conformation (like svDHFR and myDHFR) and the protein might be denatured at pressures above a few hundred megapascals. In this regard, mjDHFR might be an exception because it is very unstable in the apo-form. Highly flexible conformations may be a characteristic strategy of deep-sea proteins to adapt to high-pressure environments.

As shown above, DHFRs from deep-sea bacteria have some interesting characteristics in the primary structure, enzyme kinetics and pressure-dependence of their function. Although the tertiary structure and the enzyme reaction mechanism of these DHFRs are unknown, the present study provides good insights to better understand the pressure-adaptation mechanisms and the molecular evolution of deep-sea proteins. Further characterization of other deep-sea DHFRs is in progress to confirm whether the pressure-dependent enzyme kinetics is related to the deep-sea environment and the optimal-growth pressure of the bacteria. Although these experiments may prove to be challenging, X-ray and NMR analyses of tertiary structure,

compressibility measurements and enzyme kinetics under high pressure will help elucidate the detailed characteristics of deep-sea DHFRs.

Funding
Grant-in-Aid for Scientific Research from the Ministry of Education, Science, Sports and Culture of Japan (No. 16657031 for K.G.).

Conflict of interest
None declared.

References

1. Yayanos, A.A., Dietz, A.S., and Van Boxtel, R. (1979) Isolation of a deep-sea barophilic bacterium and some of its growth characteristics. *Science* **205**, 808–810
2. Kato, C., Sato, T., and Horikoshi, K. (1995) Isolation and properties of barophilic and barotolerant bacteria from deep-sea mud samples. *Biodiversity and Conservation* **4**, 1–9
3. Nogi, Y., Kato, C., and Horikoshi, K. (1998) Taxonomic studies of deep-sea barophilic *Shewanella* strains and description of *Shewanella violacea* sp. nov. *Arch. Microbiol.* **170**, 331–338
4. Nakasone, K., Ikegami, A., Kawano, H., Kato, C., Usami, R., and Horikoshi, K. (2002) Transcriptional regulation under pressure conditions by RNA polymerase sigma54 factor with a two-component regulatory system in *Shewanella violacea*. *Extremophiles* **6**, 89–95
5. Nakasone, K., Yamada, M., Qureshi, M.H., Kato, C., and Horikoshi, K. (2001) Piezoresponse of the *cyo*-operon coding for quinol oxidase subunits in a deep-sea piezophilic bacterium, *Shewanella violacea*. *Biosci. Biotechnol. Biochem.* **65**, 690–693
6. Tamegai, H., Kawano, H., Ishii, A., Chikuma, S., Nakasone, K., and Kato, C. (2005) Pressure-regulated biosynthesis of cytochrome *bd* in piezo- and psychrophilic deep-sea bacterium *Shewanella violacea* DSS12. *Extremophiles* **9**, 247–253
7. Chikuma, S., Kasahara, R., Kato, C., and Tamegai, H. (2007) Bacterial adaptation to high pressure: a respiratory system in the deep-sea bacterium *Shewanella violacea* DSS12. *FEMS Microbiol. Lett.* **267**, 108–112
8. Kawano, H., Nakasone, K., Matsumoto, M., Yoshida, Y., Usami, R., Kato, C., and Abe, F. (2004) Differential pressure resistance in the activity of RNA polymerase isolated from *Shewanella violacea* and *Escherichia coli*. *Extremophiles* **8**, 367–375
9. Kawano, H., Nakasone, K., Abe, F., Kato, C., Yoshida, Y., Usami, R., and Horikoshi, K. (2005) Identification of *rpoBC* genes encoding for beta and beta' subunits of RNA polymerase in a deep-sea piezophilic bacterium, *Shewanella violacea* strain DSS12. *Biosci. Biotechnol. Biochem.* **69**, 575–582
10. Bartlett, D., Wright, M., Yayanos, A.A., and Silverman, M. (1989) Isolation of a gene regulated by hydrostatic pressure in a deep-sea bacterium. *Nature* **342**, 572–574
11. Bartlett, D.H., Chi, E., and Wright, M.E. (1993) Sequence of the *ompH* gene from the deep-sea bacterium *Photobacterium* SS9. *Gene* **131**, 125–128
12. Bartlett, D.H., Kato, C., and Horikoshi, K. (1995) High pressure influences on gene and protein expression. *Res. Microbiol.* **146**, 697–706
13. Delong, E.F., Franks, D.G., and Yayanos, A.A. (1997) Evolutionary relationships of cultivated psychrophilic and barophilic deep-sea bacteria. *Appl. Environ. Microbiol.* **63**, 2105–2108
14. Bartlett, D.H. (2002) Pressure effects on *in vivo* microbial processes. *Biochim. Biophys. Acta* **1595**, 367–381
15. Chi, E. and Bartlett, D.H. (1993) Use of a reporter gene to follow high-pressure signal transduction in the deep-sea bacterium *Photobacterium sp.* strain SS9. *J. Bacteriol.* **175**, 7533–7540
16. Chi, E. and Bartlett, D.H. (1995) An *rpoE*-like locus controls outer membrane protein synthesis and growth at cold temperatures and high pressures in the deep-sea bacterium *Photobacterium sp.* strain SS9. *Mol. Microbiol.* **17**, 713–726
17. Bartlett, D.H. and Welch, T.J. (1995) *ompH* gene expression is regulated by multiple environmental cues in addition to high pressure in the deep-sea bacterium *Photobacterium species* strain SS9. *J. Bacteriol.* **177**, 1008–1016
18. Welch, T.J. and Bartlett, D.H. (1998) Identification of a regulatory protein required for pressure-responsive gene expression in the deep-sea bacterium *Photobacterium species* strain SS9. *Mol. Microbiol.* **27**, 977–985
19. Vezzi, A., Campanaro, S., D'Angelo, M., Simonato, F., Vitulo, N., Lauro, F.M., Cestaro, A., Malacrida, G., Simionati, B., Cannata, N., Romualdi, C., Bartlett, D.H., and Valle, G. (2005) Life at depth: *Photobacterium profundum* genome sequence and expression analysis. *Science* **307**, 1459–1461
20. Kato, C., Li, L., Nogi, Y., Nakamura, Y., Tamaoka, J., and Horikoshi, K. (1998) Extremely barophilic bacteria isolated from the Mariana Trench, Challenger Deep, at a depth of 11,000 meters. *Appl. Environ. Microbiol.* **64**, 1510–1513
21. Nogi, Y. and Kato, C. (1999) Taxonomic studies of extremely barophilic bacteria isolated from the Mariana Trench and description of *Moritella yayanosii sp. nov.*, a new barophilic bacterial isolate. *Extremophiles* **3**, 71–77
22. Nogi, Y., Kato, C., and Horikoshi, K. (1998) *Moritella japonica sp. nov.* a novel barophilic bacterium isolated from a Japan Trench sediment. *J Gen. Appl. Microbiol* **44**, 289–295
23. Ogawa, K., Sonoyama, T., Takeda, T., Ichiki, S., Nakamura, S., Kobayashi, Y., Uchiyama, S., Nakasone, K., Takayama, S.J., Mita, H., Yamamoto, Y., and Sambongi, Y. (2007) Roles of a short connecting disulfide bond in the stability and function of psychrophilic *Shewanella violacea* cytochrome c_5. *Extremophiles* **11**, 797–807
24. Saito, R., Kato, C., and Nakayama, A. (2006) Amino acid substitutions in malate dehydrogenases of piezophilic bacteria isolated from intestinal contents of deep-sea fishes retrieved from the abyssal zone. *J. Gen. Appl. Microbiol.* **52**, 9–19
25. Kitahara, R., Sareth, S., Yamada, H., Ohmae, E., Gekko, K., and Akasaka, K. (2000) High Pressure NMR reveals active-site hinge motion of folate-bound *Escherichia coli* dihydrofolate reductase. *Biochemistry* **39**, 12789–12795
26. Ohmae, E., Tatsuta, M., Abe, F., Kato, C., Tanaka, N., Kunugi, S., and Gekko, K. (2008) Effects of pressure on enzyme function of *Escherichia coli* dihydrofolate reductase. *Biochim. Biophys. Acta* **1784**, 1115–1121
27. Ohmae, E., Kubota, K., Nakasone, K., Kato, C., and Gekko, K. (2004) Pressure-dependent activity of dihydrofolate reductase from a deep-sea bacterium *Shewanella violacea* strain DSS12. *Chem. Lett.* **33**, 798–799

28. Ohmae, E., Iriyama, K., Ichihara, S., and Gekko, K. (1996) Effects of point mutations at the flexible loop glycine-67 of *Escherichia coli* dihydrofolate reductase on its stability and function. *J. Biochem.* **119**, 946–953
29. Fierke, C.A., Johnson, K.A., and Benkovic, S.J. (1987) Construction and evaluation of the kinetic scheme associated with dihydrofolate reductase from *Escherichia coli*. *Biochemistry* **26**, 4085–4092
30. Dawson, R.M.C., Elliot, D.C., Elliot, W.H., and Jones, K.M. (1969) *Data for Biochemical Research*, Oxford University Press, Oxford
31. Penner, M.H. and Frieden, C. (1985) Substrate-induced hysteresis in the activity of *Escherichia coli* dihydrofolate reductase. *J. Biol. Chem.* **260**, 5366–5369
32. Stone, S.R. and Morrison, J.F. (1982) Kinetic mechanism of the reaction catalyzed by dihydrofolate reductase from *Escherichia coli*. *Biochemistry* **21**, 3757–3765
33. Williams, J.W., Morrison, J.F., and Duggleby, R.G. (1979) Methotrexate, a high-affinity pseudosubstrate of dihydrofolate reductase. *Biochemistry* **18**, 2567–2573
34. Gekko, K., Kunori, Y., Takeuchi, H., Ichihara, S., Kodama, M., and Iwakura, M. (1994) Point mutations at glycine-121 of *Escherichia coli* dihydrofolate reductase: important roles of a flexible loop in the stability and function. *J. Biochem.* **116**, 703–710
35. Ohmae, E., Sasaki, Y., and Gekko, K. (2001) Effects of five-tryptophan mutations on structure and function of *Escherichia coli* dihydrofolate reductase. *J. Biochem.* **130**, 439–447
36. Ohmae, E., Fukumizu, Y., Iwakura, M., and Gekko, K. (2005) Effects of mutation at methionine-42 of *Escherichia coli* dihydrofolate reductase on stability and function: implication of hydrophobic interactions. *J. Biochem.* **137**, 643–652
37. Kuwajima, K., Garvey, E.P., Finn, B.E., Matthews, C.R., and Sugai, S. (1991) Transient intermediates in the folding of dihydrofolate reductase as detected by far-ultraviolet circular dichroism spectroscopy. *Biochemistry* **30**, 7693–7703
38. Arai, M., Maki, K., Takahashi, H., and Iwakura, M. (2003) Testing the relationship between foldability and the early folding events of dihydrofolate reductase from *Escherichia coli*. *J. Mol. Biol.* **328**, 273–288
39. Xu, Y., Feller, G., Gerday, C., and Glansdorff, N. (2003) *Moritella* cold-active dihydrofolate reductase: are there natural limits to optimization of catalytic efficiency at low temperature? *J. Bacteriol.* **185**, 5519–5526
40. Hay, S., Evans, R.M., Levy, C., Loveridge, E.J., Wang, X., Leys, D., Allemann, R.K., and Scrutton, N.S. (2009) Are the catalytic properties of enzymes from piezophilic organisms pressure adapted? *ChemBioChem* **10**, 2348–2353
41. Howell, E.E., Villafranca, J.E., Warren, M.S., Oatley, S.J., and Kraut, J. (1986) Functional role of aspartic acid-27 in dihydrofolate reductase revealed by mutagenesis. *Science* **231**, 1123–1128
42. Cameron, C.E. and Benkovic, S.J. (1997) Evidence for a functional role of the dynamics of glycine-121 of *Escherichia coli* dihydrofolate reductase obtained from kinetic analysis of a site-directed mutant. *Biochemistry* **36**, 15792–15800
43. Thompson, J.D., Higgins, D.G., and Gibson, T.J. (1994) CLUSTAL W: improving the sensitivity of progressive multiple sequence alignment through sequence weighting, position-specific gap penalties and weight matrix choice. *Nucleic Acids Res.* **22**, 4673–4680
44. Bystroff, C., Oatley, S.J., and Kraut, J. (1990) Crystal structure of *Escherichia coli* dihydrofolate reductase: The $NADP^+$ holoenzyme and the folate-$NADP^+$ ternary complex. Substrate binding and a model for the transition state. *Biochemistry* **29**, 3263–3277